https://doi.org/10.48048/tis.2024.8297

Optimizing the Pore Structure and Geometry of Polycaprolactone/Graphene Scaffold to Promote Osteogenesis

Silvia Anitasari[1,2,*], Hendrik Setia Budi[3], Yung-Kang Shen[4], Sinar Yani[5] and Nataniel Tandirogang[2]

[1]Department of Dental Material and Devices, Dentistry Program, Faculty of Medicine, Universitas Mulawarman, Samarinda 75119, Indonesia
[2]Department Medical Microbiology, Medical Program, Faculty of Medicine, Universitas Mulawarman, Samarinda 75119, Indonesia
[3]Department of Oral Biology, Faculty of Dental Medicine, Universitas Airlangga, Surabaya 60132, Indonesia
[4]School of Dental Technology, College of Oral Medicine, Taipei Medical University, Taipei 11031, Taiwan
[5]Department of Oral Biology, Dentistry Program, Faculty of Medicine, Universitas Mulawarman, Samarinda 75119, Indonesia

([*]Corresponding author's e-mail: silvia.anitasari@fk.unmul.ac.id)

Received: 11 April 2024, Revised: 9 June 2024, Accepted: 2 July 2024, Published: 10 October 2024

Abstract

Introduction: Pore structure and geometry are crucial in scaffold development for tissue engineering. From this viewpoint, pore geometry characterization methods will aid in understanding the influence of pore structure (pore size and diffusivity) on its properties. These properties determine how oxygen and water enter the scaffold, forming adsorption states. Previous studies showed that the addition of graphene (G) to polycaprolactone (PCL) increased the pore size, and played a significant role in tissue regeneration. Therefore, this study aimed to evaluate pore structure, geometry, and viability that are suitable for osteogenesis. Materials and methods: Morphology, size, and size distribution of PCL and PCL/G scaffolds were measured at concentrations of 1, 2, and 3 wt% G for the pore structure, while the connectivity of the scaffold's pore was analyzed using the geodesic tortuosity. This is essential because these factors promote the viability of osteogenesis-supporting cells. Results and discussion: The results showed that 3 wt% G had a good water diffusivity rate, larger pores, better connectivity, and viability than other concentrations. Conclusion: In conclusion, the presence of G in scaffolds affects the pore geometry and structure. This results in several advantageous effects that support osteogenesis, such as increased water and nutrient uptake, enhanced waste metabolism transport, and increased viability of the cells.

Keywords: Polycaprolactone, Graphene, Pore structure, Pore geometry, MG-63, Viability cells, Osteogenesis

Introduction

Polycaprolactone (PCL) is a polymer that is biocompatible and biodegradable, except for its mechanical properties, resulting in high suitability for various applications in the biomedical field [1]. The incorporation of graphene (G) into PCL has been shown to enhance the mechanical properties of the

polymer and improve its osteogenic capability. This signifies the importance of PCL/G in scaffold fabrication and tissue regeneration [2]. The size and arrangement of pores within the scaffold play a significant role in determining the transport of nutrients and waste products, as well as its mechanical properties. By carefully designing these pores, optimal nutrient flow and waste removal can be ensured, eventually leading to better tissue regeneration outcomes [2,3].

The pore structure has a significant impact on transport properties and functionality. It affects various processes such as fluid flow, gas diffusion, adsorption, and chemical reactions [4,5]. Pore geometry refers to the specific shape and arrangement of pores within the material. It is influenced by how the pores are arranged and interconnected, which affects diffusivity and determines the ease of fluid flow through the material [6-8].

In various fields, including filtration, catalysis, gas storage, and drug delivery, understanding pore geometry, such as geodesic tortuosity is essential. Geodesic tortuosity refers to the degree to which a path deviates from being straight [9,10]. It is commonly used as a visual tool to study the connectivity of pore networks. In addition, it is a reliable indicator of diffusive behavior, which is crucial for assessing cell biocompatibility [1,11].

The goal of optimizing the porous structure and geometry in materials is to enhance performance in various applications. The enhancements comprise designing and controlling factors such as pore size distribution, interconnectivity, overall structure, and geometry to achieve desired properties. By optimizing these parameters, the material can support the adhesion, proliferation, and differentiation of cells (osteoblast-like cells) [12]. It is particularly important in tissue engineering due to the influence of the pore on cell behavior. Therefore, this study can support cellular processes in applications such as tissue engineering.

Materials and methods

Material

The PCL/G scaffolds were produced using PCL (Mn: 80,000) from Sigma, USA, chloroform (Honeywell, USA), and sodium chloride (Sigma-Aldrich, USA), along with deionized water for fabricating PCL and PCL/G. The biocompatibility assessment was carried out using Dulbecco's Modified Eagle Medium (Gibco-Invitrogen, USA), fetal bovine serum (Gibco-Invitrogen, USA, Cat), trypsin EDTA (Gibco-Invitrogen, USA), penicillin-streptomycin (Gibco-Invitrogen, USA), and L/D cell imaging kit (Gibco-Invitrogen, USA) [13].

Manufacture of the scaffold

The solvent casting and particle leaching technique was used to manufacture scaffolds composed of PCL and PCL/G. PCL was dispersed in chloroform for 12 h at ambient temperature and various amounts of G and NaCl were then mixed with the blend for 2 h. The graphite intercalation compound was then transferred into a prepared crucible for 60 seconds in a furnace running at 700 °C to produce G. Ultrasonication was then used to disperse the synthesized G in a solvent, with the product allowed to cure at ambient temperature overnight. Chloroform also underwent a 24-h evaporation process at 37 °C within a drying vacuum oven (Deng Yng, Taiwan). Porogen removal from the scaffold was achieved by rinsing it with deionized (DI) water in a water bath (BH-130D, Taiwan) and replacing the water every 2 h. Subsequently, the scaffold was dried for 12 h at 50 °C in the oven [1,13].

Pore structure

Scanning electron microscopy (Hitachi, Japan) with a 15 kV accelerating voltage was used to examine the scaffold morphology and pore sizes. Image-J software was used to assess the pores in scanning electron microscopy (SEM) images. To estimate pore sizes, scale bars representing known distances were placed within the SEM image. Additionally, the contour of a pore was delineated and measured in micrometers (μm), with various cross-sections transported from the scaffolds [14,15].

Geodesic tortuosity

The point-wise geometric tortuosity is defined as the average of the actual flow path length. It was measured with Eq. (1):

$$r = L_e/L \tag{1}$$

where L_e is the length of the effective routes, while L is the shortest route length of the porous medium in the direction of macroscopic flow. The data was then analyzed using Matlab software (MATLAB® R2023a, USA) [16].

Extract scaffold preparation and cell seeding

The surface area of scaffolds used in the experiment was measured with Eq. (2):

$$Total\ Surface\ Area = 2\pi rh\ x\ 2\pi \tag{2}$$

where π is 3.14, r is the radius, and h is the height. A scaffold was placed in a 50 mL sterile conical polypropylene centrifuge tube (Falcon, USA). DMEM supplemented with 10 % FBS and 1 % penicillin/streptomycin was then added with the formula Eq. (3):

$$Total\ Medium\ (mL) = (Total\ Surface\ Area)/6) \tag{3}$$

and shaken in a water bath (BH-130D, Taiwan) at 37 °C and 100 rpm for 24 h. The extract of PCL/G scaffolds was sterilized and filtered with a 0.22 μm Millipore filter unit (Sartorius, France) and a polyethersulfone (PES) membrane [17].

Osteoblast-like (MG-63) cells (at passage 5) were cultured in 96-well plates with DMEM containing 10 % FBS and 1 % penicillin in an incubator at 37 °C with 5 % CO_2 for 24 h. Each well was seeded with 100 μL of an extract of a PCL/G scaffold and incubated. After incubation for 24 h, a live-dead assay was performed following the manufacturer's instructions (Invitrogen, USA) [18,19].

Live/dead (L/D) assay

The L/D cytotoxicity assay was conducted on scaffolds seeded with cells after 24 h, following the guidelines provided by the manufacturer. An L/D cell imaging kit containing component A (stains live cells green) and component B (stains dead cells red), were combined to create a 2× working solution. After removing DMEM from each well, scaffolds were washed with 1x Phosphate-Buffered Saline (PBS) twice. Within 2 h, an equal volume (100 μL) of 2× working solution was then added to cells in each 96-well microplate and incubated for 15 min at 20 - 25 °C. The top surface of a scaffold was observed using a cell imaging inverted fluorescence microscope (IX73 inverted microscopes, Olympus, Japan) with

excitation/emission (CooILED's pE-300 lite, Olympus, Japan) of 488/515 nm (live green) and 570/602 nm (dead red). In addition, the standard filter set was FITC or green fluorescent protein (GFP; live green), and Texas red (red dead). Live and dead cell images were processed and combined using Bio Tek Gen 5.0 software (Agilent, Santa Clara, USA) images taken at random from the 96-microplate culture well, and cell density was evaluated using FIJI software [20,21].

Statistical evaluation

The mean and standard error (SE) were used to present the experiment data for each sample group in this study. To ensure statistical validity, all experiments were conducted with at least 3 scientific replicates and the data obtained were analyzed using the SAS program. To determine significant differences between groups, a one-way analysis of variance (ANOVA) was performed on normally distributed. If the data did not meet the assumptions of normality, the Kruskal-Wallis ANOVA was used.

To evaluate the differences between groups, Tukey's post hoc test was used for ANOVA-analyzed, while the Mann-Whitney significant difference post hoc test was used for Kruskal-Wallis-analyzed data. In addition, the significance levels were set at $*p < 0.05$, $**p < 0.01$, $***p < 0.00$, and $****p < 0.0001$ [7,19].

Results and discussion

The study showed that the incorporation of 3 wt% G in the PCL scaffold resulted in a more favorable distribution of pore sizes compared to other concentrations and PCL ($p < 0.0001$). Specifically, the percentage of pore sizes less than 100 μm showed comparable results to the 1 wt% G concentration, and PCL exhibited a distribution where the percentage of pore size greater than 501 μm exceeded that of the pore sizes between 301 - 500 μm. This unfavorable distribution hindered the adhesion and proliferation of MG-63 cells and other cell types such as fibroblasts and endothelial cells shown in **Table 1**.

Table 1 Pore size distribution of PCL and PCL/G.

Scaffold	< 100 μm $\bar{X}$ ± SE	*p*-value	101 - 300 μm $\bar{X}$ ± SE	*p*-value	301 - 500 μm $\bar{X}$ ± SE	*p*-value	> 5001 μm $\bar{X}$ ± SE	*p*-value
PCL	100.2 ± 0.6		59.8 ± 0.8		18.0 ± 0.4		24.5 ± 0.4	
1 wt% G	303.0 ± 1.6	****	73.8 ± 0.9	****	18.5 ± 0.8	****	17.3 ± 0.4	0.000
2 wt% G	119.8 ± 2.0	[a]	54.5 ± 0.4	[a]	14.3 ± 0.6	[a]	5.3 ± 0.4	[a]
3 wt% G	100.7 ± 0.8		74.3 ± 0.6		30.3 ± 0.4		8.2 ± 0.3	

[a] $p < 0.0001$. Abbreviation: $\bar{X}$, mean; SE, standard error.

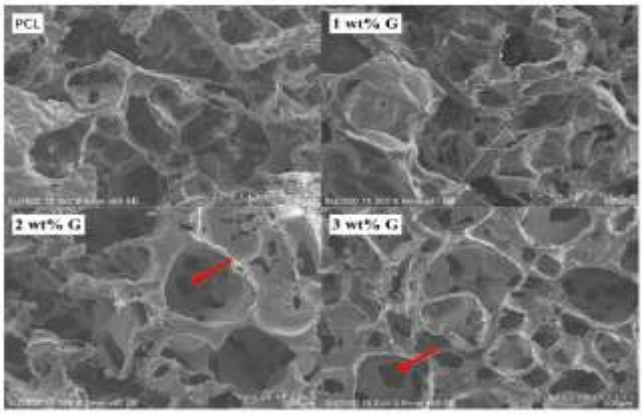

Figure 1 Pore morphology and distribution of PCL and PCL/Graphene scaffold at 1, 2, and 3 wt% G. It showed the interconnection pore in the large pore at 2 and 3 wt% G (red arrow).

The SEM examination in **Figure 1** confirmed the interconnection feature of the pores and provided insights into the pore size distribution. The image showed that the 2 and 3 wt% G concentrations had better interconnectivity compared to PCL and 1 wt% G (red arrow). This may be due to pore sizes of these concentrations being larger than < 100 µm. According to a study by Jia *et al.* [22], it is known to enhance interconnectivity. In contrast, PCL and 1 wt% G had smaller pore sizes, which resulted in less effective interconnection.

Various materials are being studied as potential substitutes for lost bone tissue. However, only a limited number have demonstrated satisfactory outcomes, encouraging the use of synthetic materials as a feasible alternative. In the field of bone tissue engineering, a combination of inorganic and organic materials derived from both natural and synthetic polymers is used. Scaffolds are also made up of both natural and synthetic polymers [23].

The findings from this study indicate that a PCL/G scaffold with 3 wt% G concentration had a favorable pore size distribution, particularly in the range of 101 - 300 µm. This pore size range is known to promote osteoblast growth, which is crucial for bone tissue formation. It should be emphasized that osteoblasts are typically 50 µm in size, while fibroblasts range from 10 to 15 µm. Furthermore, for fibroblast ingrowth and osteoblast proliferation the scaffold pore size should be smaller than 100 µm and larger than 101 µm, respectively [22,23].

Other studies have shown that microspores of 10 µm are essential for enhancing osteoinduction, even though pore sizes below 100 µm cause the development of non-mineralized osteoid fibrous tissues [1]. These tissues promote cytokine production by fibroblasts, leading to increased osteoclast multiplication, inhibition of osteoblast functions, and local inflammation. Therefore, achieving the optimal balance of pore sizes in a scaffold is essential for promoting the desired cell differentiation and tissue formation [8,24].

In this study, the geodesic tortuosity factor remained the same for PCL and PCL/G scaffolds, while the diffusivity differed among the different G concentrations. The porous scaffold with 3 wt% G exhibited higher diffusivity compared to the scaffolds with 1 and 2 wt% G. This can be attributed to the presence of a higher number of pores with sizes greater than 101 µm in the 3 wt% G scaffold, as shown in **Figure 2** and **Table 2**. Larger pore sizes facilitate better fluid flow through the scaffold, leading to higher diffusivity.

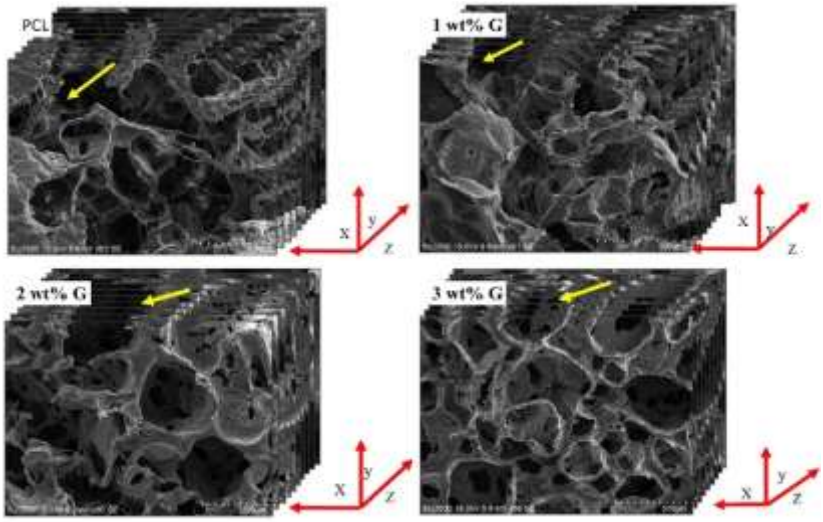

Figure 2 Map of Representative Volume Analysis (RVA) from 22 to 100 % (cubic) of PCL and PCL/G scaffolds. The slices were milled in the z-direction, while y represents the direction of diffusive transport. The channel pores are shown in white (yellow arrow).

Table 2 Geodesic tortuosity factor and diffusivity of the PCL and PCL/G scaffolds.

Scaffold	Diffusivity (m^2s^{-1})	*p*-value	Geodesic tortuosity factor (τ)	*p*-value
PCL	0.439 ± 0.00	* [a]	1.04	ns
1 wt% G	0.417 ± 0.01		1.04	
2 wt% G	0.437 ± 0.00		1.04	
3 wt% G	0.441 ± 0.00		1.04	

[a] $p < 0.05$; ns: non- significant.

Geodesic tortuosity is a crucial parameter used to describe porous materials and their flow characteristics. Diffusivity is a single parameter that describes the flow paths within a porous medium. It shows the complexity of the medium and measures the resistance to fluid flow [25]. The complexity of porous media refers to how convoluted or tortuous the flow paths are within the material. Highly porous media have intricated, winding paths that impede the movement of fluids, particles, or electrons. Furthermore, it is a significant factor in determining the resistance of the medium to various types of flow, such as fluid flow, electrical current, or mass diffusion [8,26].

The architecture of interconnected pores in multiple channels has a significant impact on cell proliferation, differentiation, and the formation of bone tissue *in vivo* [27]. These findings suggest that the improved architecture initiates a bone formation process without requiring additional biological components such as cells. The channels enable fluid movement and generate consistent fluid shear, which cells can detect. This, in turn, triggers mechano-transduction signaling pathways associated with cell growth and tissue development [5,28]. Therefore, pore geometry and pore size of scaffolds have a significant impact on cell differentiation and tissue formation. The scaffold surface exhibited evenly distributed and interconnected pores with sizes ranging between 200 and 400 μm. It influenced the flow diffusivity within the material, which directly affects the cellular response and the formation of bone-like tissue. This study suggests that controlling and optimizing the pore geometry of the scaffold can influences the quantity and structure of the engineered tissue, wherever, the fluid flow generated by the scaffold's pore structure is essential for promoting cell differentiation and directing the deposition of minerals [26,29].

The results of the live/dead assay in **Figure 3**(**A**) shows the osteoblast-like MG-63 cells to be better proliferated on the 3 wt% concentrations of G than the other concentrations and PCL. This result was confirmed by taking images of the MG-63 cells and analyzing for cell densities of live and dead cells in the scaffold after 24 h. On PCL scaffolds, an average of 516 (± 159) cells/mm^2 were observed as live cells, with 754 (± 86) cells/mm^2 as dead cells. On 1 wt% G scaffolds, live cells were 2110 (± 97) cells/mm^2 and 358 (± 106) cells/mm^2 were dead cells. On 2 wt% G scaffolds, 2386 (± 135) cells/mm^2 were live cells and 118 (± 25) cells/mm^2 were dead, and on 3 wt% G scaffolds were 2537 (± 81) cells/mm^2 as live cells, with 53 (± 3) cells/mm^2 as dead cells. The data revealed that PCL/G scaffolds with various G concentrations had higher viability than PCL scaffolds ($p \leq 0.001$) with 3 wt% G scaffolds exhibiting a smaller density of dead cells than the others ($p \leq 0.05$) and up to 5-fold fewer compared to PCL scaffolds ($p \leq 0.001$) after 24 h (**Figure 3**(**B**)).

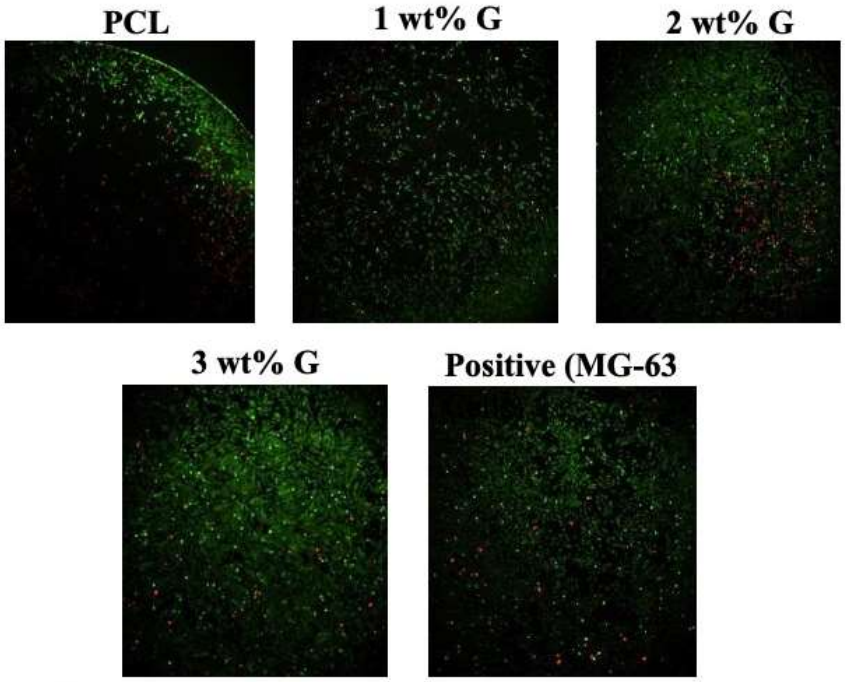

(A)

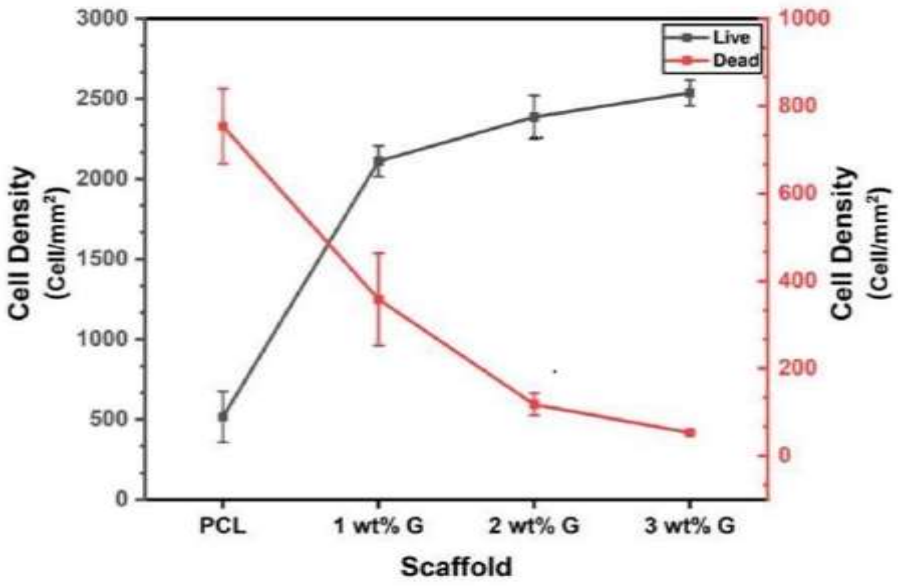

(B)

Figure 3 Live/dead cell assay. (A) live (cells illuminated by green light)/dead (cells illuminated by red light) assay after 24 h; (B) Cell density of PCL and PCL/G scaffolds after 24 h; ****p-value < 0.0001 compared to PCL (live cells); *$p < 0.05$ compared to PCL (dead cells).

The fluid flow induced by the pore geometry of the scaffold plays a crucial role in stimulating cell differentiation and guiding the mineral deposition process. These insights emphasize the importance of tailoring scaffold properties for enhanced tissue engineering outcome. In addition, porous architecture with increased vascular diffusivity is essential for successful reconstruction [20]. Although pore size and volume are important factors influencing bone ingrowth and formation, pore geometry, including uniformity,

orientation, and interconnectivity is also a key design consideration. An interconnected architecture allows for the penetration of body fluids and cells, facilitating bone ingrowth. Even at the same pore size and volume, pore geometry can significantly impact osteoconduction. For instance, in this study, it was found that the incorporation of 3 wt% G in the PCL scaffold resulted in a scaffold with high interconnected pores. These interconnected pores had a larger pore size with a diameter greater that 101 μm. This is in contrast to other concentrations and PCL, which had smaller pore s size. The presence of larger pores (> 101μm) is favorable for osteoblast proliferation, promoting bone ingrowth, and rapid bone regeneration, as shown in **Figure 3(A)**. Therefore, the PCL/G scaffold with a concentration of 3 wt% G shows promise for tissue engineering applications requiring these specific characteristics [7].

The presence of different pore sizes in a scaffold can lead to variations in the tortuosity of the pore space. In this study, the tortuosity value remained the same despite the different pore sizes, while the diffusivity of the scaffold differed. This suggests that the size of the pore became more complex, causing fluid or cells to take shorter routes or bypass larger pores. As shown in **Figure 2**, an increase or decrease in the deviation of pore size can directly impact the average value of tortuosity in the scaffold [9,30].

Conclusions

In conclusion, the scaffold with a concentration of 3 wt% G had larger pores (> 100 μm) and better interconnectivity, which is favorable for osteoblast adhesion, proliferation, and differentiation. In the tortuosity and diffusivity analysis of the scaffolds, the size of the pores played a role in fluid flow and diffusivity. The scaffold with 3 wt% G exhibited higher diffusivity compared to the scaffolds with 1 and 2 wt% G. This was probably due to the larger pore sizes in the 3 wt% G scaffold. Overall, the results suggest that pore size and geometry are essential factors to consider when designing scaffolds for application in tissue engineering.

Acknowledgments

The authors are grateful to Muhammad Romadhon for providing valuable assistance in the laboratory of dental materials and devices throughout this study.

References

[1] S Anitasari, C Wu and Y Shen. PCL/Graphene scaffolds for the osteogenesis process. *Bioengineering* 2023; **10**, 305.

[2] E Batoni, AF Bonatti, CD Maria, K Dalgarno, R Naseem, U Dianzani, CL Gigliotti, E Boggio and G Vozzi. A computational model for the release of bioactive molecules by the hydrolytic degradation of a functionalized polyester-based scaffold. *Pharmaceutics* 2023; **15**, 815.

[3] O Faruq, S Sayed, B Kim, S Im and B Lee. A biohasic calcium phosphate ceramic scaffold loaded with oxidized cellulose nanofiber-gelatin hydrogel with immobilized simvastatin drug for osteogenic differentiation. *J. Biomed. Mater. Res. B Appl. Biomater.* 2020; **108**, 1229-38.

[4] S Mandal, Viraj, S Nandi and M Roy. Effects of multiscale porosity and pore interconnectivity on *in vitro* and *in vivo* degradation and biocompatibility of Fe-Mn-Cu scaffolds. *J. Mater. Chem. B* 2021; **9**, 4340-54.

[5] D Martinez-Moreno, G Jimenez, C Chocarro-Wrona, E Carrillo, E montanez,C Galocha-Leon, B Clares-Naveros, P Galvez-Martin, G Rus, JD Vicente and JA marchal. Pore geometry influences growth and cell adhesion of infrapatellar mesenchymal stem cells in biofabricated 3D thermoplastic scaffolds useful for cartilage tissue engineering. *Mater. Sci. Eng. C* 2021; **122**, 111933.

[6] P Prochor and A Gryko. Numerical analysis of the influence of porosity and pore geometry on functionality of scaffolds designated for orthopedic regenerative medicine. *Materials* 2021; **14**, 109.

[7] X Wang, Z Nie, J Chang, ML Lu and Y Kang. Multiple channels with interconnected pores in a bioeramic scaffold promote bone tissue formation. *Sci. Rep.* 2021; **11**, 20447.

[8] CJ Bullock and C Bussy. Biocompatibility considerations in the design of graphene biomedical materials. *Adv. Mater. Interfaces* 2019; **6**, 1900229.

[9] Y Yao, Y Yang, Q Ye, S Cao, X Zhang, K Zhao and Y Jian. Effects of pore and porosity on cytocompatibility and osteogenic differentiation of porous titanium. *J. Mater. Sci. Mater. Med.* 2021; **32**, 72.

[10] WL Roque and RRA Costa. A plugin for computing the pore/grain network tortuosity of a porous medium from 2D/3D micro CT image. *Appl. Comput. Geosci.* 2020; **5**, 100019.

[11] A Lin, S Liu, L Xiao, Y Fu, C Liu and Y Li. Controllable preparation of bioactive open porous microspheres for tissue engineering. *J. Mater. Chem. B* 2022; **10**, 6464-71.

[12] S Anitasari, HS Budi, Y Shen and YMD Arina. New insight of scaffold based on hydroxyapatite (HAp)/bacteria's nanocellulose (BN) for dental tissue engineering. *Eur. J. Dent.* 2024; **18**, 891-7.

[13] H Huang, F Fan, Y Shen, C Wang, Y Huang, M Chern, Y ang ang L Wang. 3D poly-ε-caprolactone/graphene porous scaffolds for bone tissue engineering. *Colloids Surf. A* 2020; **606**, 125393.

[14] HS Budi, S Anitasari, Y Shen, M Tangwattanachuleeporn, P Nuraini and NA Setiabudi. Novel application of 3D scaffolds of poly (E-caprolactone)/graphene as oasteoinductive properties in bone defect. *Eur. J. Dent*. 2023; **17**, 790-6.

[15] M Tahriri, MD Monico, A Moghanian, MY Yaraki, R Torres, A Yadegari and L Tayebi. Graphene and its derivatives: opportunisties and challenges in dentistry. *Mater. Sci. Eng. C* 2019; **102**, 171-85.

[16] A Tripathi and A Pandey. Post-hoc comparison in survival analysis: An easy Approach. *J. Biosci. Med*. 2017; **5**, 112-9.

[17] JM Unagolla and AC Jayasuriya. Enhanced cell functions on graphene oxide incorporated 3D printed polycaprolactone scaffolds. *Mater. Sci. Eng. C Mater. Biol. Appl.* 2019; **102**, 1-11.

[18] CSD Cabral, SP Miguel, DD Melo-Diogo, RO Loura and IJ Correia. Green reduced graphene oxide functionalized 3D printed scaffolds for bone tissue engineering, Carbon. *Carbon* 2019; **146**, 513-23.

[19] A Kimura, H Abe, S Tsuruta, S Chiba, Y Fujii-Kuriyama, T Sekiya, R Morita and A Yoshimura. Aryl hydrocarbon receptor protects against bacterial infection by promoting macrophage survival and reactive oxygen species production. *Int. Immunol*. 2014; **26**, 209-20.

[20] M Furuya, J Kikuta, S Fujimori, S Seno, H Maeda, M Shirazaki, M Uenaka, H Mizuno, Y Iwamoo, A Morimoto, K Hashimoto, T Ito, Y Isogai, MKashii, T Kaito, S Ohba, U Chung, AC Lichtler, KKikuchi, H Matsuda, ..., M Ishii. Direct cell-cell contact between mature osteoblast and osteoclast dynamically controls their functions *in vivo*. *Nat. Commun*. 2018; **9**, 300.

[21] V Sokolova, L Rojas-Sanchez, N Bialas, N Schulze and M Epple. Calcium phosphate nanoparticle-mediated transfection in 2D and 3D mono- and co-culture cell models. *Acta Biomater*. 2019; **84**, 391-401.

[22] G Jia, H Huang, J Niu, C Chen, J Weng, F Yu, D Wang, B Kang, T Wang, G Yuan and H Zeng. Exploring the interconnectivity of biomimietic hierarchical porous Mg scaffolds for bone tissue engineering: Effect of pore size distribution on mechanical properties, degradation behavior and cell migration ability. *J. Magnesium Alloys* 2021; **9**, 1954-66.

[23] M Janmohammadi, MS Nourbakhsh, M Bahraminasab and L Tayebi. Effect of pore characteristics

and alkali treatment on the physicochemical and biological properties of a 3D-printed polycaprolactone bone scaffold. *ACS Omega* 2023; **8**, 7378-94.

[24] M Elsheikh, R Kishida, K Hayashi, A Tsuchiya, M Shimabukuro and K Ishikawa. Effects of pore interconnectivity on bone regeneration in carbonate apatite blocks. *Regener. Biomater.* 2022; **9**, rbac010.

[25] Y Chen, JE Frith, A Dehghan-Manshadi, H Attar, D Kent, NDM Soro, MJ Bermingham and MS Dargusch. Mechanical properties and biocompatibility of porous titanium scaffolds for bone tissue engineering. *J. Mech. Behav. Biomed*. *Mater*. 2017; **75**, 169-74.

[26] T Shabab, O Bas, B Dargaville, A Ravichandran, PA Tran and DW Hutmacher. Microoporous/macroporous polycaprolactone scaffolds for dental applications. *Pharmaceutics* 2023; **15**, 1340.

[27] MB Mazalan, MAB Ramlan, JH Shin and T Ohashi. Effect of geometric curvature on collective cell migration in tortuos microchannel devices. *Micromachines* 2020; **11**, 659.

[28] A Naini. Physical characterization and analysis of tissue inflammatory response of the combination of hydroxyapatite gypsum puger and tapioca starch as a scaffold material. *Dent. J.* 2023; **56**, 53-7.

[29] RA Ferdynanto, PES Dewi, PTK Dharmayanti and W Prananingrum. The effect of various concentrations of HA-TCP derived from cockle shell synthesis on scaffold porosity. *Dent. J.* 2018; **51**, 114-8.

[30] K Ghosal, P Mondal, S Bera and S Ghosh. Graphene family nanomaterials-opportunities and challenges in tissue engineering applications. *FlatChem* 2021; **30**, 100315.